

A306

## ATOMIZATION CHARACTERISTICS OF A DOUBLE IMPINGING F-O-O-F TYPE INJECTOR WITH FOUR STREAMS FOR LIQUID ROCKETS

Shin-Jae Kang\*, Byung-Joon\*\*, Jae-Youn Jung\*\*, Je-Ha Oh\*\*\* and Ki-Chul Kwon\*\*\*\*

- \* Faculty of Mechanical Engineering, Chonbuk National University, and AHTRI, Chonbuk, Korea  
 \*\* Faculty of Mechanical Engineering, Chonbuk National University, and NAHTEC, Chonbuk, Korea.  
 \*\*\* Chonbuk Automobile Part and Mold TIC, Chonbuk National University, Chonbuk, Korea  
 \*\*\*\* Graduate School, Chonbuk National University, Chonbuk, Korea

**ABSTRACT** This paper presents atomization characteristics of a double impinging F-O-O-F type injector with four streams. A phase doppler particle analyzer was employed to measure the droplet-size and water was used as the inert simulant liquid instead of reactive propellant liquids. The droplet mean diameter(SMD) and size distribution were measured to investigate the effects of the momentum ratio of fuel and oxidizer. The SMD distribution appeared to be the largest at  $MR=2.12(r=2.00)$ . The difference between  $\overline{SMD}$  at  $x=50\text{mm}$  and at  $x=100\text{mm}$  reduces as the momentum ratio increases. Droplet size distributions measured in the impinging spray flow field coincide well with all size distribution functions. MMD and  $D_{0.632}$  decrease as the momentum ratio increases. This experimental results can be used at the preliminary design stage of an impinging stream type injector for the liquid rockets.

**Keywords:** Liquid rocket fuel injector, Impinging type, Phase Doppler Particle Analyzer(PDPA), Sauter Mean Diameter(SMD), Momentum Ratio(MR)

### 1. INTRODUCTION

To develop a liquid rocket engine, analysis should be validated with experimental data. Fluid dynamic and thermodynamic phenomena in a combustion chamber of the engine affect the performance of the propulsion system. Therefore, the combustion chamber performance should be estimated accurately to develop liquid rocket engines. The element closely related to the combustion chamber performance is the propellant injector because it affects the mixing performance, atomization, and spatial distribution of propellant.

Many types of liquid rocket fuel injectors have been developed. In this study, the impinging type injector, which makes the propellant impinge on each other and produces impinging energy, was investigated. In the early work, Elverum et al.(1959) investigated empirically the optimum mixing distributions of propellants in an impinging type liquid rocket injector. Rupe(1956) also studied a correlation between the dynamic properties of a pair of impinging streams and the uniformity of mixture ratio distribution in the resulting sprays. Calhoun et al.(1973) suggested an injector design model for predicting rocket engine performance. This model quantifies the combustion performance and chamber heat flux as functions of injector element type, element area ratio, impingement angle, mixture ratio, momentum ratio, and physical size. Also, design equations are given for combustion performance evaluation in injectors. Brault and Lourme(1985) carried out cold flow tests for characterization of Viking rocket 'line-on-line' injectors based on the extension of a Malvern sizer. Hulka and Schneider(1993) carried out the cold flow

testing of an oxidizer-swirled coaxial single element injector in the Space Transportation Main Engine(STME). In their study, increasing the oxidizer injection velocity had greatest influence on reducing oxidizer droplet size parameters and increasing the size distribution for non-gas assisted flows. Rho et al.(1998) also investigated the droplet velocity, turbulence flow properties, mean droplet size distribution, and droplet rate in a two-phase swirling jet using a Phase Doppler Particle Analyzer (PDPA) system.

Santoro et al.(1995) studied the performance of a swirl coaxial injector with various mixing conditions. Park et al.(1994) investigated the spray characteristics of an impinging doublet injector. The atomization characteristics of scaled-down versions of a coaxial rocket injector and a quadruplet rocket injector were investigated using a PDPA by Sankar et al.(1991). Specifically, they presented the effects of the gas pressure and the injector recess size on flow variables such as the mean droplet diameter, Sauter mean diameter, number density, volume flux, and droplet velocity. Rho et al.(1995) made measurements on the atomization characteristics, and derived an expression that there would be pertinent droplet size distribution functions and an absolute correlation between the SMD and mass ratio.

This paper presents atomization characteristics of a double impinging F-O-O-F type injector with four streams. Propellant is atomized and mixed by impinging energy. The double impinging type injector sprays fuel in outward two jets and oxidizer in inward two jets through the orifice. Water was used in lieu of fuel and oxidizer. The atomized droplet size as well as the three dimensional axial velocity components were measured using a Phase Doppler Particle

Analyzer (PDPA).

## 2. TEST FACILITIES AND EXPERIMENTAL ARRANGEMENT

Test facilities are composed of a simulant propellant feeding system, an injector and a laser measurement system.

The propellant feeding system delivers propellant from the propellant tank to the injector. An industrial displacement pump was employed to supply the propellant continuously to the injector at high pressure and flow rate. This pump can provide a maximum discharge flow rate of 99 l/min and a maximum discharge pressure of 60 kgf/cm<sup>2</sup>. In addition, a ball valve, which can resist high pressures, was used to control the flow rate. The supply pressure was measured just before the simulant propellant was provided to the injector.

The injector is an F-O-O-F type in which the outward two fuel jets impinge onto inward two oxidizer jets. Thus, the propellant is mixed and atomized.

The specification of the uni-element injector applied in this study is shown in Fig. 1 and Table 1.

Fuel is injected through the orifices ① and ④ and oxidizer through the orifices ② and ③. The fuel stream through orifice ① initially impinges onto the oxidizer stream from ②. (③ impinges onto ④) These impinged jets impinge again and then form the impinging sprays.

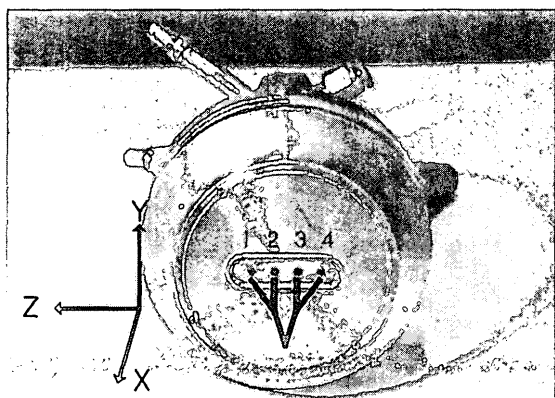


Fig. 1 The shape and dimensions of injector

Table 1 Design values of injector

Type	Double impinging type [F-O-O-F TYPE]
First impinging angle( $\theta_1$ )	30°
First impinging length	10.39mm
Oxidizer orifice diameter	2.2mm
Fuel orifice diameter	1.6mm

The first impinging length is the distance from the center of the orifice exit plane to the point where the centers of the fuel and oxidizer streams first impinge. When the impinging length is long, it causes bad atomization because the breakup length becomes long. On the other hand, when the impinging length is short, it results in a burnout of the injector plane by the wake flow. Therefore, the first impinging length was set to be 10.39 mm in this study. An impinging angle is closely related to the wake flow of propellant, the uniformity of mixture, the atomizing length of the spray, the atomized droplet size and the width of the spray. When the impinging angle is small, mixture becomes better but the impinging length becomes long. When the impinging angle is large, atomized droplet size becomes small but the wake flow of mixed propellant increases and causes the burnout of the injector plane. As a result, the impinging angle was determined within a range applied ordinarily in the impinging injector.

Three dimensional Phase Doppler Particle Analyzer(PDPA) was employed to measure the atomized droplet size and velocity components.

Water was used instead of propellant liquids. Atomized droplet size was measured for various oxidizer/fuel ratios. The total flow rate was fixed at 260g/s. A change of a momentum ratio means a change in the mixture ratio( $r=m_o/m_f$ ). Table 2 shows the experimental conditions.

When the momentum ratio was changed, the droplet size was measured at the axial distance of 20 mm, 30 mm, 50 mm and 100 mm. Each cross section has 21×21 measurement points.

Table 2 Spray conditions

(Unit m : g/s, P : kPa)					
r	MR	$m_f$	$m_o$	$P_f$	$P_o$
1.50	1.19	104.0	156.0	725.3	532.5
2.00	2.12	86.70	173.3	503.5	657.7
2.47	3.22	75.00	185.0	377.1	749.5
3.00	4.76	65.00	195.0	283.2	832.2
3.50	6.48	57.80	202.2	223.8	895.0

## 3. RESULTS AND DISCUSSION

The impinging injector used in this study has a considerable droplet size compared with other types of injectors since it has a large orifice diameter and a high flow rate unlike the others such as pressure atomizer.

The droplet size distributions are depicted in Fig. 2 for the momentum ratio of fuel and oxidizer under the fixed total flow rate at 260 g/s. As seen from the cross section at  $x=20$  mm,  $x=30$  mm and  $x=50$  mm in Fig. 2, there is an unmeasured area near the center of the spray. It is assumed that the causes would be the effects of high mass flux of the

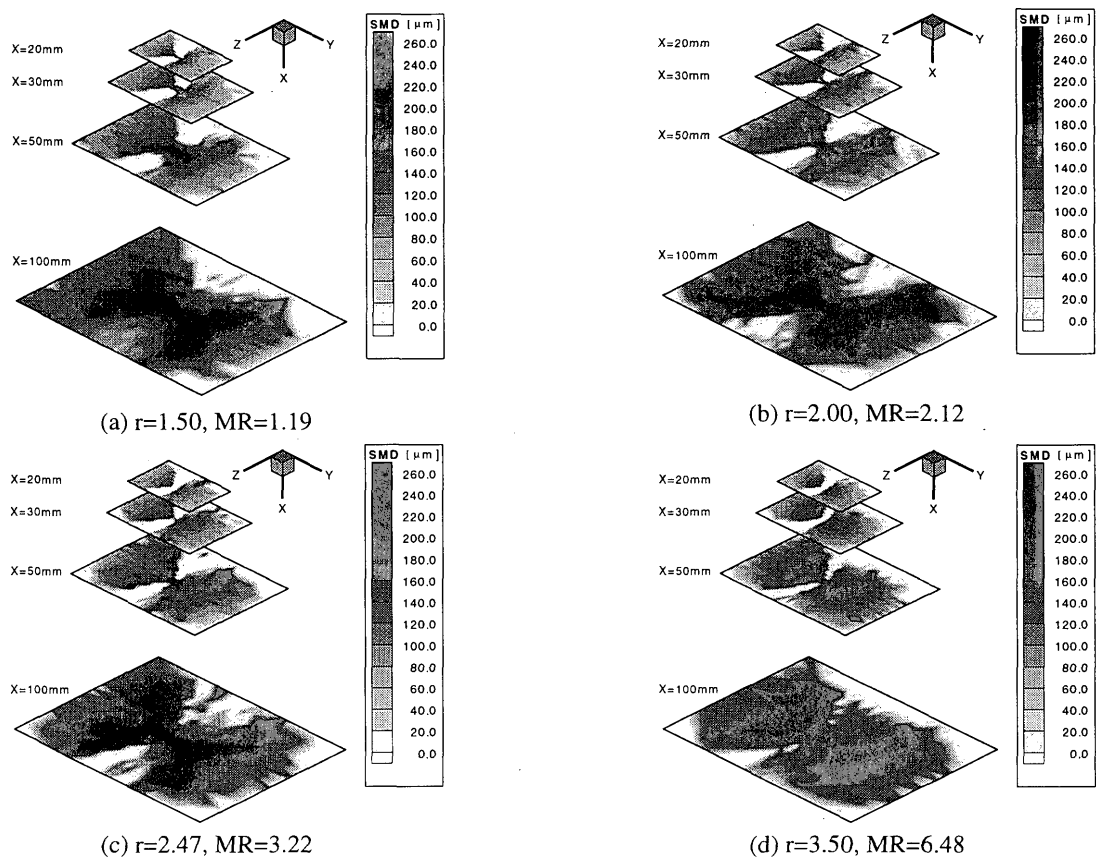


Fig. 2 Iso-drop size(SMD) contours with momentum ratio

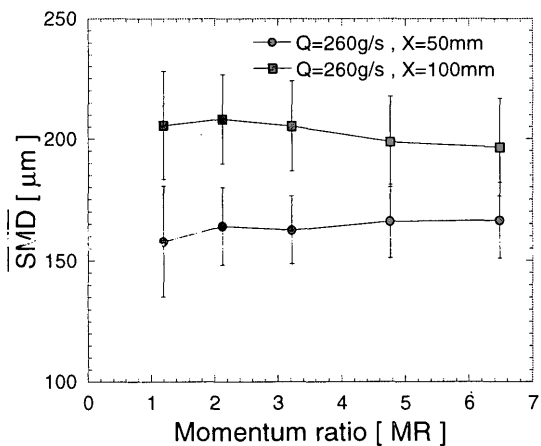


Fig. 3 Variation in mean droplet size(  $\overline{SMD}$  ) with momentum ratio

spray flow field and impinging jets in a liquid sheet condition unsplit to droplets. Figure 2 shows that the SMD of droplets increases, as the distance of axial locations becomes long. The SMD of droplets increases for momentum ratios between 1.19 and 2.12. However, it declines for momentum ratios between 2.12 and 6.48. The former result occurs because the momentum decrease of

outer fuel jets have an influence on the spilt of droplets more than the momentum increase of inner oxidizer jets. The latter result is due to the momentum increase of inner jets. However, the SMD becomes larger near the center of the spray as the momentum ratio increases. The reason for this is that the spilt of droplets is processing in the center of the spray because the breakup length increases on account of the effect of the momentum increase of inner jets.

Figure 3 shows the mean values of SMD at every point for  $x=50\text{ mm}$  and  $x=100\text{ mm}$  away from the injector plane. While the  $\overline{SMD}$  at  $x=50\text{ mm}$  generally increases as the momentum ratio goes up, the  $\overline{SMD}$  at  $x=100\text{ mm}$  decreases. The maximum  $\overline{SMD}$  occurs at  $x=100\text{ mm}$ , when the momentum ratio is 2.12. These results are similar to Kang's result (1999) in which the SMD of droplets was measured for various momentum ratios of oxidizer and fuel under the fixed total flow rate. According to Kang (1999), the  $\overline{SMD}$  of droplets increases for momentum ratios between 0.64 and 1.78, but it decreases for momentum ratios above 1.78. The results from this study suggest that the  $\overline{SMD}$  increases for momentum ratios between 1.78 and 2.12, and that it declines for momentum ratios above 2.12. Therefore, when momentum ratios are changed under the fixed total flow rate, these trends are satisfied. However, the momentum ratio should be neither high nor low. When the momentum of inner streams is low, it is likely to affect the spray flow field badly because of the wake flow.

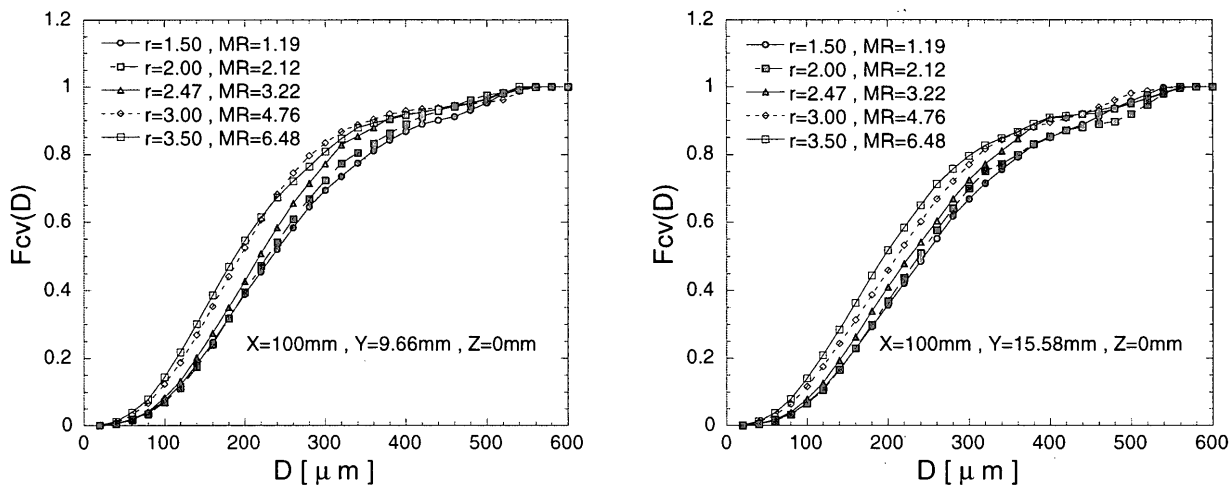
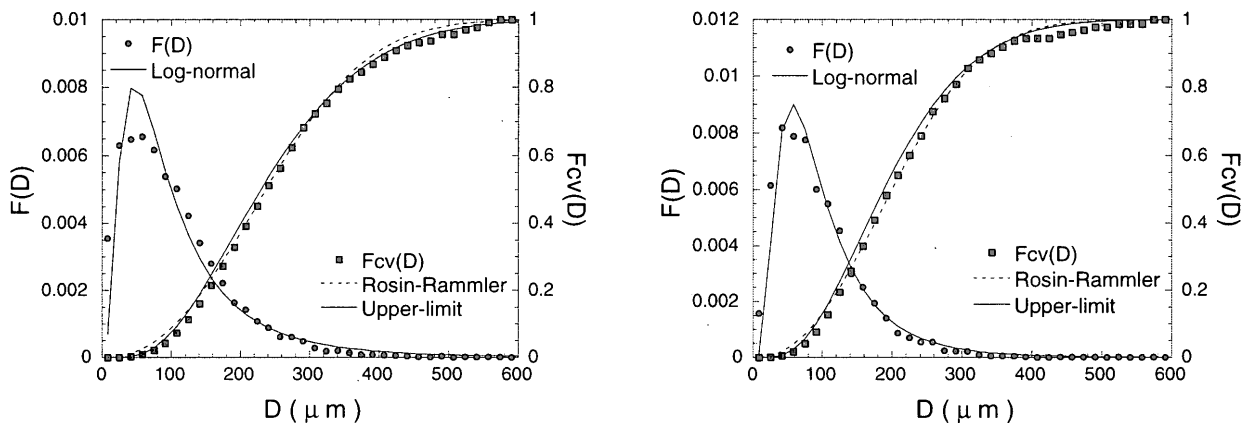


Fig. 4 Droplet size distribution



(a)  $r=1.50, x=100\text{mm}, y=4.5\text{mm}, z=0\text{mm}$

(b)  $r=3.50, x=100\text{mm}, y=4.5\text{mm}, z=0\text{mm}$

Fig. 5 Droplet size distribution function

The latter occurs because the inner jets do not go completely to the axial location after impinging onto the outer jets at the exit plane. When the momentum of inner streams is high, the spray form will likely be similar to the pressure atomizer and atomization will likely be dependant on the pressure drop variation of the inner jets. This is because the outer jets cannot break through the inner jets. Thus, only two inner jets proceed.

Moreover, the  $\Delta SMD$  ( $SMD_{x=100\text{mm}} - SMD_{x=50\text{mm}}$ ) declines as the momentum ratio increases (Fig. 3). This is because the momentum increase of inner streams results in the small reduction of inertia force, as droplets move to the axial direction.

Graphics of the cumulative volume distribution vs momentum is shown in Fig. 4. The Rosin-Rammler distribution function (Rosin and Rammler, 1939) and the Upper-limit distribution function (Mugele and Evans, 1951), which are used frequently to express a droplet size distribution mathematically, are obtained from the using measured droplet size distributions. The measured droplet size distribution is compared with the Rosin-Rammler

distribution function and the Upper-limit distribution function, as shown in Fig. 5.

As shown in Fig. 4,  $D_{0.632}$ ,  $X$ , and  $D_{0.5}$  which presents mass median diameter (MMD) increase as the momentum ratio increase. The cumulative volume taken up by small droplets also increases as the momentum ratio increases, but it is the least when the momentum ratio is 2.12.

In Fig. 5, the cumulative volume distributions of measured droplets are compared with the Rosin-Rammler distribution function and the Upper-limit distribution function. The Number distribution is also compared with the Log-normal distribution function. According to Fig. 5, the cumulative volume distribution of measured droplets match with the Rosin-Rammler distribution function and the Upper-limit distribution function. The Number distribution and the Log-normal distribution function also match.

However, when the droplet size section is divided into small, medium and large parts, the Upper-limit distribution function coincides well in small and large part. However, it inclines to the left in the medium part where

MMD and  $D_{0.632}$  are included. On the other hand, the Rosin-Rammler distribution function does not match in small and large parts, but it does well in the medium part. The Upper-limit distribution function coincides well in small and large parts because it finds the appropriate value using a trial-and-error method, which assumes the maximum and the minimum value of droplets. The Rosin-Rammler distribution function matches well in MMD and  $D_{0.632}$  because  $D_{0.632}$  is the significant variable of the Rosin-Rammler distribution function.

For the Log-normal distribution function and the Number distribution which presents density of probability of measured droplet size, droplets which have the maximum density of probability comparatively coincide. However, the maximum density of probability calculated by the Log-normal distribution function is higher than the measured maximum density of probability.

#### 4. CONCLUSIONS

The study investigated the atomization characteristics of the double impinging F-O-O-F type injector by changing the pressure drop variation and the momentum ratio. The results are as follows.

The SMD of droplets decreases as the momentum ratio of fuel and oxidizer increases when the total flow rate is fixed. In addition, the SMD distribution appeared to be the largest at  $MR=2.12(r=2.00)$ . The difference between  $\overline{SMD}$  at  $x=50\text{mm}$  and at  $x=100\text{mm}$  reduces as the momentum ratio increases. The SMD and the  $\overline{SMD}$  in the cross sections for the momentum ratio variation are similar. It is believed that the mean values of all SMD at every point in the cross sections,  $\overline{SMD}$  is better to investigate the atomization characteristics than the local SMD at one point.

Droplet size distributions measured in the impinging spray flow field coincide well with the Upper-limit distribution function in small and large size ranges. Droplet size distributions match with the Rosin-Rammler distribution function in the medium size range where MMD and  $D_{0.632}$  exist. MMD and  $D_{0.632}$  decrease as the momentum ratio increases.

#### REFERENCE

1. Brault, F. and Lourme, D., Experimental Characterization of the Spray Formed by Two Impinging Jets in Liquid Rocket Injector, ONERA TP No. 1985-68. (1985)
2. Calhoon, D. F., Kors, D. L. and Gordon, L. H., An Injector Design Model for Predicting Rocket Engine Performance and Heat Transfer, AIAA Paper 73-1242. (1973)
3. Elverum, G. W. and Morey, T., Criteria for Optimum Mixture Ratio Distribution Using Several Types of Impinging Stream Injector Elements, Memorandum 30-5, Jet Propulsion Lab. Calif. Inst. Tech. (1959)
4. Hulka, J. and Schneider, J. A., Single Element Injector Cold Flow Testing for STME Swirl Coaxial Injector Element Design, AIAA, SAE, ASME, and ASEE, Joint Propulsion Conference and Exhibit, 29th, Monterey, CA. (1993)
5. Huzel, D. K. and Huang, Modern Engineering for Design of Liquid-Propellant Rocket Engines, AIAA, Washington, (1992) pp. 104 ~ 115.
6. Kang, S. J., Oh, J. H., Park, S. M., Kwon, K. C., and Che, Y. S., An Experimental Study on Spray Characteristics of Impinging Type Injector for Liquid Rocket, Proceeding of the KSAS 1999 Spring Annual Meeting, (1999) pp. 314 ~ 317.
7. Lefebvre, A. H., Atomization and Spray, Hemisphere Publishing Co., (1989) pp. 79 ~ 103.
8. Mugele, R. and Evans, H. D., Droplet Size Distribution in Sprays, Ind. Eng. Chem., Vol. 43, No. 5, (1951) pp. 1317 ~ 1324.
9. Park, S. Y., Kim, S. J., Park, S. W. and Kim, Y., A Study on Spray Characteristics of the Triplet Impinging Stream Type Injector for Liquid Rocket, Transactions of KSME, Vol. 20, No. 3, (1996) pp. 1005 ~ 1014.
10. Rho, B. J., Kang, S. J., and Oh, J. H., An Experimental Study on the Atomization Characteristics of a Two-Phase Turbulent Jet of Liquid Sheet Type Co-Axial Nozzle, Transactions of KSME, Vol. 19, No. 6, (1995) pp. 1529 ~ 1538.
11. Rho, B. J., Kang, S. J., Oh, J. H., and Lee, S. G., Swirl Effect on the Spray Characteristics of a Twin-Fluid Jet, KSME International Journal, Vol. 12, No. 5, (1998) pp. 899 ~ 906.
12. Rosin, P. and Rammler, E., The Laws Governing the Finess of Powered Coal, J. Inst. Fuel, Vol. 7, No. 31, (1939) pp. 29 ~ 36.
13. Rupe, J. H., A Correlation Between the Dynamic Properties of a Pair of Impinging Streams and the Uniformity of Mixture Ratio Distribution in the Resulting Spray, Prog. Rep. 20-209, Jet Propulsion Lab. Calif. Inst. Tech. (1956)
14. Sankar, S. V., Brenadalarosa, A., Isakovic, A., and Bachalo, W. D., Experimental Investigation of Rocket Injector Atomization, The 28th JANNAF Combustion Subcommittee Meeting, (1991) Vol. 2, pp. 187 ~ 198.
15. Santoro, R. J., Pal S., and Rahman, Swirl Coaxial Atomization; Cold-Flow and Hot-Fire Experiments, AIAA 95-0381 (1995)
16. Sutton, G. P. and Ross, D. M., Rocket Propulsion Elements, (1976) John Wiley & Sons, Inc., USA, pp. 286 ~ 295.